Desert Research Institute

Remote Sensing of Evapotranspiration at the Nevada Environmental Response Trust Site and Nearby Properties

Matt Bromley
Blake Minor
Chuck Russell
Justin Huntington
Kelsey Carrara

July 2023

Publication No. 41296

Prepared by
Division of Hydrologic Sciences, Desert Research Institute

Prepared for
Nevada Division of Environmental Protection

THIS PAGE LEFT INTENTIONALLY BLANK

Remote Sensing of Evapotranspiration at the Nevada Environmental Response Trust Site and Nearby Properties

Matt Bromley
Blake Minor
Chuck Russell
Justin Huntington
Kelsey Carrara

July 2023

Publication No. 41296

Prepared by
Division of Hydrologic Sciences, Desert Research Institute

Prepared for
Nevada Division of Environmental Protection

THIS PAGE LEFT INTENTIONALLY BLANK

CONTENTS

LIST OF FIGURES

LIST OF TABLES

LIST OF ACRONYMS

ASCE	American Society of Civil Engineers
BMM	Beamer-Minor method
BR	Bowen ratio
CEMP	Community Environmental Monitoring Program
CI	confidence interval
DEM	digital elevation model
DRI	Desert Research Institute
E	evaporation
EBC	energy balance closure
EBR	energy balance ratio
EC	eddy covariance
ET	evapotranspiration
ET*	normalized ETa
ETa	actual evapotranspiration
ETg	groundwater evapotranspiration

ETM+	Enhanced Thematic Mapper Plus
ETo	grass reference evapotranspiration
FAO	Food and Agriculture Organization
GIS	geographic information system
IDW	inverse-distance weighting
LaSRC	Landsat Surface Reflectance Code
LEDAPS	Landsat ecosystem disturbance adaptive processing system
LST	land surface temperature
MNDWI	Modified Normalized Difference Water Index
NAIP	National Agriculture Imagery Program
NDEP	Nevada Department of Environmental Protection
NDVI	Normalized Difference Vegetation Index
NDWI	Normalized Difference Water Index
NDWR	Nevada Department of Water Resources
NERT	Nevada Environmental Response Trust
NIR	near infrared
OLI	Operational Land Imager
PAGD	potential areas of groundwater discharge
PI	prediction interval
PPT	precipitation
QA/QC	quality assurance and quality control
RAWS	Remote Automated Weather Station
SEB	surface energy balance
SWIR	short wave infrared
TM	Thematic Mapper (TM)
USGS	U.S. Geological Survey

THIS PAGE LEFT INTENTIONALLY BLANK

ABSTRACT

The Las Vegas Wash ("the Wash") is an important surface-water body within the Las Vegas Valley. The Wash has been highly affected by resource management activities and modification of the hydraulic flow. Adjacent areas have been highly affected by urban development and industrial activity. This impact is most evident at the Nevada Environmental Response Trust site (the former Tronox LLC site), where the groundwater in the area has been contaminated by perchlorates, chromium, and other compounds (Ramboll, 2019). To guide remediation efforts currently managed by Ramboll, improved groundwater contaminate transport modelling was required. Because evapotranspiration (ET) from phreatophytic vegetation is a primary component of groundwater discharge, improved ET data could improve the accuracy of modeling activities.

This effort was guided by year-specific delineations of phreatophyte and surface water extent that were necessary to characterize the significant changes to vegetation extent and composition, urban development, and management of the Las Vegas Wash. This study applied a regression-based approach that was developed for the areas within the state of Nevada. Similar approaches have been used throughout the region and are well suited for this application. The use of gridded meteorological data and both optical and thermal remote sensing data allows for the development of a historical time series of data, which could not be produced with the collection of in situ measurements or by traditional methods.

This study developed 26 years of data describing rates and volumes of groundwater ET (ETg), actual ET (ETa), and evaporation by water year, defined as October 1st to September 30th of the following year. The rates of ETg ranged from 1.35 ft/yr to 2.22 ft/yr, the rates of ETa ranged from 1.65 ft/yr to 2.52 ft/yr, and shallow water evaporation ranged from 6.91 to 8.85 ft/yr.

THIS PAGE LEFT INTENTIONALLY BLANK

INTRODUCTION

The Las Vegas Wash is an important geographic feature within the Las Vegas Valley. This 12-mile-long waterway is characterized as a highly modified wetland, wildlife habitat, and an urban waterway. The Las Vegas Wash conveys water from stormwater, urban runoff, shallow groundwater, and treated wastewater from nearby water treatment facilities to Lake Mead, thereby allowing for the conveyance of the excess water from the Las Vegas Valley to the Colorado River (Las Vegas Valley Water District, 2023; SNWA, 2023).

The Las Vegas Wash and the surrounding areas have been greatly affected by alterations to the waterway, management of vegetation, and urban development (Figures 1 and 2). Previous industrial activity at the Nevada Environmental Response Trust (NERT) site has resulted in contamination of the local groundwater with perchlorates and other compounds. Remediation is ongoing and has been guided by the published Phase 6 Groundwater Flow and Transport Model conducted by Ramboll (Ramboll, 2019). This modeling relied on estimates of evapotranspiration (ET) derived from field investigations and aerial image interpretation, which established the spatial extents of phreatophytic vegetation for the study period of 2014 to 2018. Groundwater discharge areas were primarily assumed for areas covered by 61 percent to 100 percent tamarisk. These spatial extents were multiplied by a fixed, annual rate of groundwater ET to arrive at annual volumetric estimates of phreatophytic ET (Ramboll, 2019).

In the Phase 6 study, quarterly rates of surface water evaporation from the Las Vegas Wash were extrapolated using typical annual rates of ET for the basin (Ramboll, 2019). These annual rates of evaporation were disaggregated based on monthly rates of evaporation calculated from instrumentation at Lake Mead (Westenburg et al., 2006). This approach may not have considered the physics present in large bodies of water, such as heat storage, which may have skewed annual patterns in assumed evaporation rates.

The overarching goal of this report is to use remote sensing methodologies in conjunction with gridded climate data to develop year-specific and site-specific estimates of water conveyed to the atmosphere through evapotranspiration and evaporation. This will include both rates and volumes of water conveyed through phreatophytic vegetation as groundwater ET (ETg) and calculated actual ET (ETa). Estimates of shallow surface water evaporation were also developed to account for evaporative losses from the Las Vegas Wash. These data will be used to improve estimates of groundwater flux and groundwater flow in perchlorate transport modeling. This effort improves on previous estimates of ET for the study area in the Phase 6 Model, as this provides improved spatial and temporal resolution of rates of groundwater ET, actual ET, and evaporation, which will improve estimates of contaminate flow and discharge in the Phase 7 groundwater flow and transport model.

METHODS

Potential Areas of Groundwater Discharge

Groundwater discharge in the Las Vegas Wash occurs primarily via bare soil evaporation and phreatophyte transpiration, which are accounted for in the combined term "evapotranspiration." Phreatophytes are plants that rely on shallow groundwater for some of their water requirements and extend their tap roots into the capillary fringe and water table (Robinson, 1958). Understanding the extent of phreatophyte vegetation is crucial to

determining potential areas of groundwater discharge (PAGD) and developing accurate estimates of ETg volumes. Although individual phreatophytes have relatively low ETg rates, their large contributing areas equate to large groundwater discharge volumes (Nichols, 2000; Smith et al., 2007; Beamer et al., 2013).

The PAGD for the Wash (1995 to 2021) were digitized in a geographic information system (GIS). Scanned plate maps delineating both natural conditions (Malmberg, 1965; Harrill, 1976) and historical phreatophyte distributions (Maxey and Jameson, 1948; Harrill, 1988) were georectified in a GIS and used to develop initial PAGD boundaries. Because of the considerable changes observed in the Wash over the study period (1995 to 2021) and in prior years, the initial boundaries needed to be modified to reflect contemporary conditions and account for interannual variations in phreatophyte extent for the 26-year study period. Datasets used to develop year-specific PAGD boundaries include the following: 1) high-resolution National Agriculture Imagery Program (NAIP) data, 2) Google Earth Pro Timelapse imagery, 3) Landsat-derived Normalized Difference Vegetation Index (NDVI) data, 4) Landsat-derived land surface temperature (LST) data, 5) a digital elevation model (DEM), 6) depth-to-groundwater measurements from observation wells and well logs, and 7) the phreatophyte extent from the Phase 6 model.

Depth-to-groundwater datasets for the Wash and surrounding areas were obtained from the Nevada Department of Water Resources (NDWR) and U.S. Geological Survey (USGS) databases. These data—combined with the initial phreatophyte distributions, DEM, midsummer Landsat imagery, and NAIP imagery—were used to modify and constrain PAGD boundaries to lowland areas where the depth to groundwater is within the typical phreatophyte limit of 50 feet (Robinson, 1958; Nichols, 1994) and areas that displayed a relatively cool surface temperature and high vegetation vigor compared with the adjacent xerophyte vegetation that occupy upland areas. Midsummer (June 1st through September 15th) median NDVI and LST composite images were computed for each year of the study period using Climate Engine (Huntington et al., 2017). The midsummer median was chosen to aggregate the Landsat data so that the peak phreatophyte vegetation vigor was characterized, the groundwater signal from phreatophytes was maximized, and the influence of late-summer monsoonal precipitation events on greenness and surface temperature was minimized. This approach attempts to isolate the signal of vegetation vigor that is the result of winter precipitation and groundwater access.

The PAGD boundaries were constrained to groundwater modeling domains developed by Ramboll, with one exception. The northern edge of the Phase 6 domain excluded portions of the PAGD. Limiting this study to a strict adherence to the Phase 6 model boundary would have resulted in the omission of phreatophytic vegetation. For this report, the Phase 6 model boundary was manually adjusted to enable the ETg estimation methods applied in this study. This issue has been addressed in the development of the Phase 7 modeling domain, where the updated modeling domain contains all areas of phreatophytic identified and delineated in this study (Alka Singhal, Ramboll, personal communication, October 21, 2022).

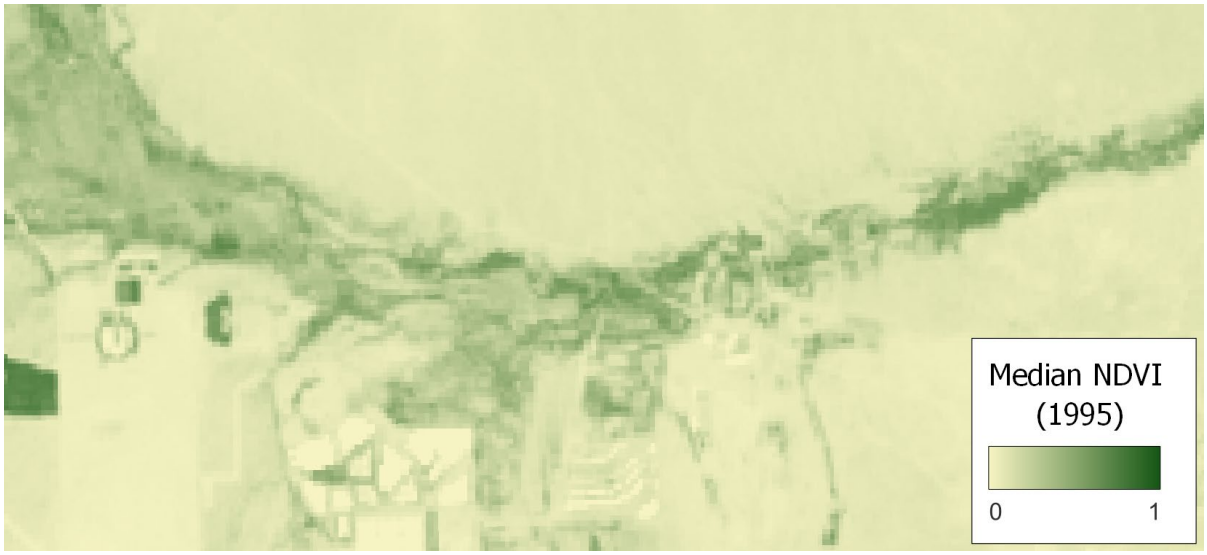

Figure 1. Median NDVI image of the Las Vegas Wash in 1995.

Figure 2. Median NDVI image of the Las Vegas Wash in 2020.

Evaluation of Meteorological Data

The methods used in this study to estimate open water evaporation and phreatophyte ET account for the atmospheric demand for moisture by using calculated grass reference ET (ETo) in a gridded data format. For this application, ETo was provided by gridMET (Abatzoglou, 2013). This dataset has the benefit of providing spatially explicit meteorological data at a daily time step for a period beginning in 1979 to the present year. These data are generated at ~4 km resolution and are calculated using the ASCE Penman-Monteith equation (Allen et al., 2005). To validate gridMET data for this specific application, a comparison was conducted using ETo calculated at in situ stations in the vicinity of the study area. However, long-term, high-quality meteorological data

representative of the study area were difficult to obtain. The station networks evaluated for use in this analysis were the Remote Automated Weather Station (RAWS) network (Zachariassen et al., 2003), the Community Environmental Monitoring Program (CEMP), and the Clark County Regional Flood network.

The RAWS stations—which are sited in locations of natural, vegetated landcover—collect the meteorological data necessary to calculate reference ET and have historically benefitted from regular maintenance. Stations from this network were excluded from the analysis in this study on the basis that station sites being considered non-representative of the study area. The primary basis for exclusions was installation sites located an excessive distance from the study area or installed at much higher elevations than the study area. The CEMP meteorological network was evaluated for suitability. However, most of these stations were excluded from the analysis based on factors involved in siting. The most common issues were stations located near pavement, buildings, air-conditioning units, etc. The Clark County Regional Flood network maintains multiple stations near the study area that were evaluated for suitability, but the typical sensor complements lacked the instrumentation necessary to calculate ETo.

The screening of meteorological stations yielded three stations that were best suited for comparison with gridMET (Figure 3 and Table 1). Weather data produced by these stations were evaluated, filtered, and corrected using a PyWeatherQAQC (*PyWeatherQAQC - Graphical Weather Data Correction — PyWeatherQAQC 0.3.0 Documentation*, n.d.), an open-source software developed at DRI that processes data according to the recommendations and guidelines of Allen (1996) and ASCE-EWRI (Allen et al., 2005). The quality assurance and quality control (QA/QC) process primarily focused on removing erroneous data and correcting measurements of solar radiation and humidity. Solar radiation was compared with theoretical limits of clear-sky solar radiation and corrections were preformed to compensate for issues such as possible dust or debris on the pyranometer window, a non-level base plate, sensor miscalibration or drift, or obstructions (Allen, 1996). Humidity measurements were examined for annual occurrences of conditions of 100 percent relative humidity and expected differences in dew point depression.

The corrected in situ weather data was used to calculate reference ET and was compared with gridMET ETo calculated using Gridwxcomp, another open-source tool developed by DRI (*WSWUP/Gridwxcomp: Comparison of Weather Station and Gridded Climate Datasets*, n.d.). The typical approach used in the application of Gridwxcomp is the development of monthly or annual bias-correction surfaces interpolated between station sites using an inverse-distance weighting interpolation. These surfaces would subsequently be multiplied by gridMET ETo to create a spatially explicit, bias corrected ETo product. Given that the Boulder City CEMP station was located much closer to the study site than the two RAWS stations used in this analysis, a bias-correction surface would have given disproportionate weight to biases documented at the Boulder City CEMP station.

The average annual bias of all stations was found to be 1.05, with an average summer bias of 1.04. In previous studies, an absolute bias in ETo of less than 15 percent indicated that gridMET was a good fit for the development of ET data (Huntington et al., 2022). Given the lack of a definitive indication of a consistent bias and the potential issues of applying an IDW interpolated bias correction surface, it was determined that ETo from gridMET would be used in its native and unaltered state.

Table 1. Summary of meteorological stations compared with gridMET to identify potential biases.

Station	Network	Location	Elevation (feet)	Date Record Started	Date Record Ended	Summer Mean Ratio (Station/gridMET)	Annual Mean Ratio (Station/gridMET)
Boulder City	CEMP	35° 59' 06", 114° 50' 29"	2713	7/1/1999	3/31/2022	0.85	0.86
Red Rock	RAWS	36° 08' 07", 115° 25' 38"	4096	6/1/1990	3/31/2022	1.04	1.05
Yucca Gap	RAWS	36° 26' 12", 115° 19' 53"	2984	9/1/2004	3/31/2015	1.23	1.25

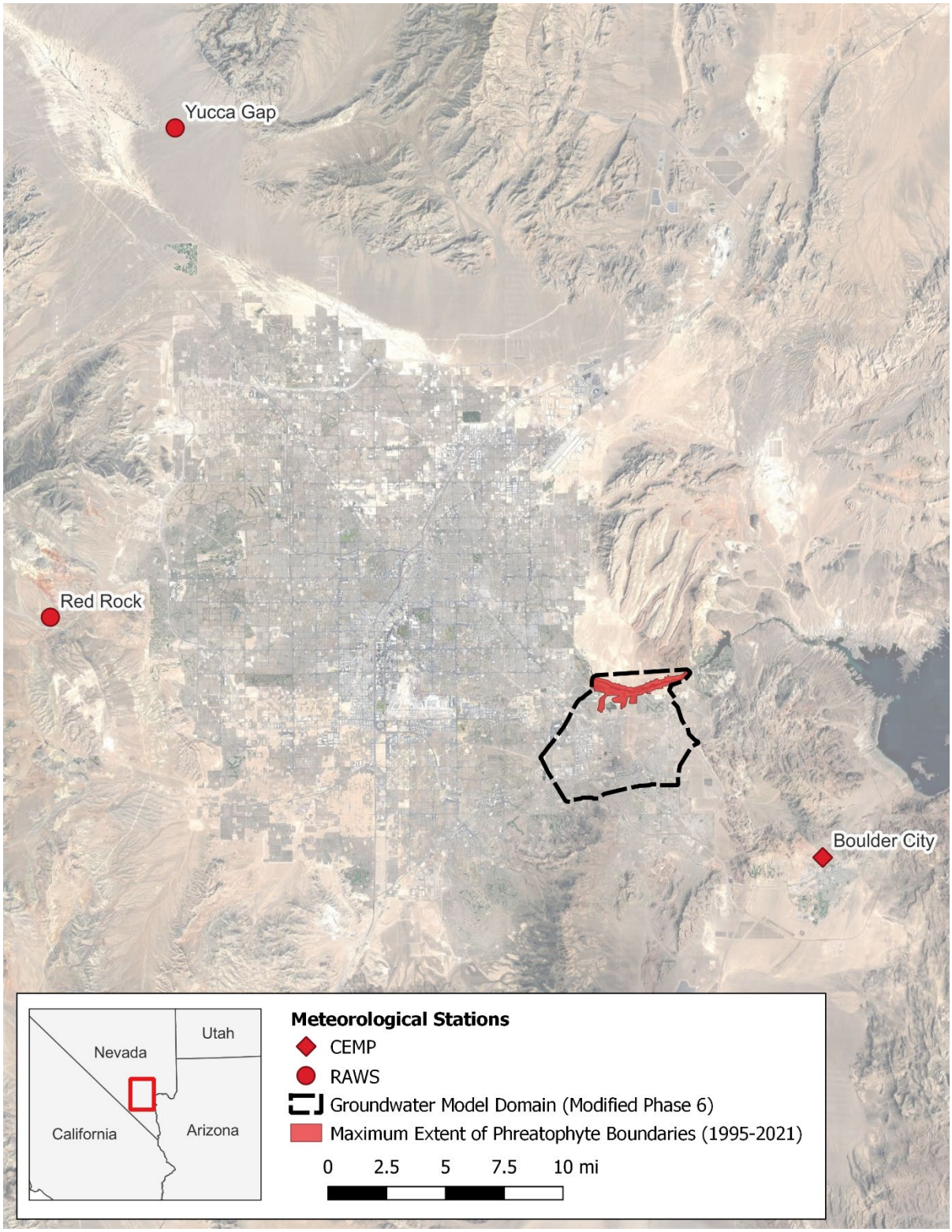

Figure 3. Overview of the Las Vegas Valley, the study area, and the relevant meteorological stations.

Evapotranspiration

Groundwater Evapotranspiration

Groundwater ET from phreatophyte vegetation in the Las Vegas Wash and the surrounding area was estimated for the study period using the Landsat satellite archive, gridded climate data from gridMET, and the collection of GIS datasets and products described previously in this report. Annual ETg rates for the wash were estimated using a revised version of the approach described by Groeneveld et al. (2007), Beamer et al. (2013), and Minor (2019), which is referred to herein as the Beamer-Minor method (BMM). The BMM approach relies on water year total ET estimates derived from in situ micrometeorological and energy balance data collected at 36 sites (54 site years; some sites collected multiple years of ET estimates) from 10 studies in the Great Basin (Allander et al., 2009; Arnone et al., 2008; Berger et al., 2016; DeMeo, 2018; DeMeo et al., 2008; Garcia et al., 2014; Maurer et al., 2005; Moreo et al., 2007, 2017; Reiner et al., 2002) and the corresponding evaporative demand and precipitation (PPT) from gridMET (Abatzoglou, 2013).

An energy balance closure (EBC) correction approach based on the energy balance ratio (EBR) similar to the FLUXNET methodology (Pastorello et al., 2020) was used to correct 39 site years of eddy covariance (EC) ET data at the daily time step, where the EBR is the ratio of the sum of turbulent fluxes (sensible heat flux and latent heat flux) to the available energy (net radiation less the soil heat flux). The other 15 site years of in situ ET data were collected using the Bowen ratio (BR) energy balance method, which inherently forces closure and does not require EBC corrections. Performing energy balance closure at the daily time step has been shown to reduce the effects of soil-heat-flux measurement inaccuracies that can occur at the sub-hourly time step (Leuning et al., 2012). Before corrections were applied, EBR values ranged from 0.62 to 1.18 with a mean EBR of 0.92 across all sites. Following EBC corrections, EBR values ranged from 0.98 to 1.02 with a mean EBR of 1.01 across all sites. Detailed processing and gap-filling steps are explained in the flux-data-qaqc GitHub repository (https://github.com/Open-ET/flux-data-qaqc).

After EBC corrections and normalization of the in situ ETa data for each site year, normalized ETa (ET*, response variable) was paired with the respective Landsat Collection 2 surface reflectance NDVI around each micrometeorological station to develop a linear least-squares regression model (Figure 4). The source area NDVI (independent variable) for each site year was computed as the spatial average of the respective midsummer median NDVI composite (using a 100-meter buffer around the station). The NDVI – ET* approach used in this study is advantageous because variations in vegetation characteristics, evaporative demand, and PPT are accounted for in both deriving and applying the relationship, which enables transferability without the need for more in situ ET data in the local area of application.

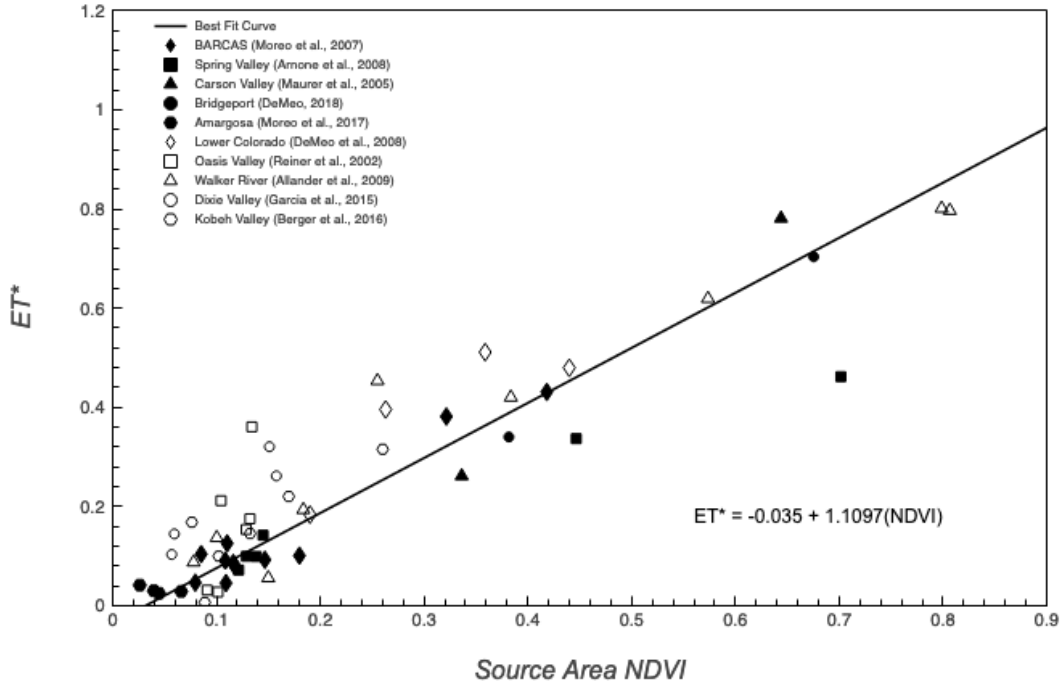

Figure 4. NDVI – ET* data pairs for 54 site years of eddy covariance and Bowen ratio flux tower stations used in the Beamer-Minor method. Symbols indicate which ET study the data point represents. The best-fit line and prediction equation are provided.

The NDVI was used in this study over other indices because it is a relatively simple formulation, commonly used among the scientific community, and has been shown to perform well for quantifying vegetation cover in arid environments (McGwire et al., 2000; Wu, 2014). The NDVI incorporates the red and near infrared (NIR) spectral bands and is defined as:

$$NDVI = \frac{(NIR - RED)}{(NIR + RED)} \qquad (1)$$

where NIR represents the near infrared surface reflectance and RED represents the red surface reflectance sourced from Landsat satellite data. The USGS converts the Landsat 5 Thematic Mapper (TM), the Landsat 7 Enhanced Thematic Mapper Plus (ETM+), and the Landsat 8 Operational Land Imager (OLI) top-of-atmosphere reflectance to surface reflectance using the Landsat ecosystem disturbance adaptive processing system (LEDAPS) (for Landsat TM and ETM+) and Landsat Surface Reflectance Code (LaSRC) (for Landsat OLI) atmospheric correction algorithms (*Landsat 8-9 Collection 2 Level 2 Science Product Guide | U.S. Geological Survey*, 2022; Schmidt et al., 2013). The NDVI ranges from ~0.03 to 0.9 over land, with higher NDVI values signifying greater vegetation vigor. Because of the slight differences in Landsat sensor bandwidths, cross-sensor calibration was applied for a continuous time series analysis of the NDVI for the study period. Cross-sensor calibration between Landsat TM, ETM+, and OLI at-surface reflectance red and NIR bands was performed using equations developed by Huntington et al. (2016) that are based on Landsat images acquired over Arizona, California, Nevada, and Utah.

As was mentioned previously, midsummer was selected as an appropriate period for aggregating Landsat NDVI imagery. The period of June 1st through September 15th was chosen to include all imagery within the period of peak phreatophyte vegetation vigor. Rigorous cloud masking and QA/QC methods were applied to ensure only the highest-quality Landsat imagery was considered in the analysis. The QA/QC steps involved computations of supplemental vegetation indices (e.g., enhanced vegetation index), water indices (e.g., normalized difference water index), LST, and albedo to assist with identifying and filtering poor-quality images. Following the removal of poor-quality imagery, normalized ET (ET*) for a given water year defined as:

$$ET^* = \frac{ETa - PPT}{ETo - PPT} \quad (2)$$

was estimated using the NDVI – ET* linear regression equation:

$$ET^* = \beta_0 + \beta_1 NDVI \quad (3)$$

where ETa is water year total actual ET in millimeters per year (mm/yr), PPT is the water year total precipitation (mm/yr), ETo is the water year total grass reference ET (i.e., evaporative demand) (mm/yr), and B0 and B1 are the best-fit regression coefficients of -0.035 and 1.1097, respectively (Figure 5; Table 2). Applying equation 3 to midsummer NDVI resulted in estimates of mean ET* with upper and lower 90th percentile confidence and prediction intervals included (Table 2). The confidence interval (CI) represents the degree of confidence in the mean ET* estimated for a given NDVI observation, whereas the prediction interval (PI) signifies the degree of confidence for a new NDVI and ET* pair to fall within the interval at the 0.10 significance level (i.e., 90th percentile). The PI is wider than the CI because it must account for the uncertainty in estimating the population mean ET*, plus the random variation of individual observations (Figure 4). By rearranging equation 2, water year ETa was estimated as:

$$ETa = (ETo - PPT)ET^* + PPT \quad (4)$$

where water year total PPT and ETo was estimated using gridMET. Water year ETg is then estimated by subtracting the water year PPT from the estimated water year ETa:

$$ETg = (ETo - PPT)ET^* \quad (5).$$

Water year ETg was estimated for year-specific PAGD boundaries from the 1995-2021 study period using the equations above with the following steps: 1) spatially averaged gridMET water year PPT and ETo for phreatophyte areas; 2) computed spatially distributed NDVI using Landsat Collection 2 surface reflectance data; 3) computed spatially distributed ET*, ETa, and ETg rates; 4) spatially averaged ETg rates; and 5) multiplied spatially averaged ETg rates by respective phreatophyte area (as defined by the PAGD boundaries) to estimate ETg volumes. All the above steps were applied to each year of the study period using all QA/QC-ed June 1st through September 15th Landsat imagery. A temporal median for each year was used to compute median NDVI, ETa, and ETg, which resulted in an annual time series of median NDVI and water year ETo, PPT, ETa, and ETg estimates from 1995 to 2021. Outputs from the analysis include tabular summaries of phreatophyte areas, water year ETg rates, water year ETg volumes (with 90th percentile CI and PI estimates included), and water year ETg rasters at a 30-meter resolution. Annual ETg rasters were further disaggregated to seasonal time steps by first computing water year

ETg/ETo ratios, and then multiplying the ETg/ETo ratio by the seasonal ETo. For each water year, the four seasons are defined as October through December, January through March, April through June, and July through September. After seasonal ETg rasters were prepared, spatial summaries were computed and attributed to the groundwater model domain grid shapefile.

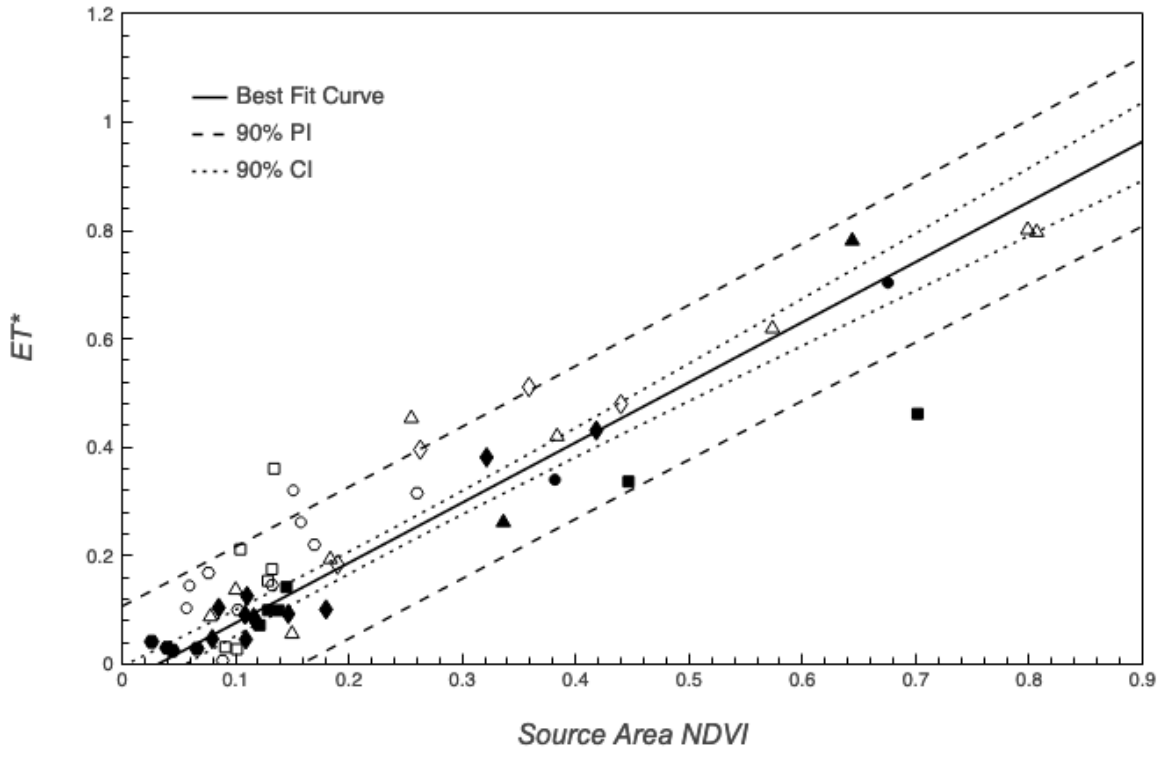

Figure 5. NDVI – ET* data pairs with the best-fit line and upper/lower 90th percentile confidence and prediction intervals.

Table 2. β-coefficients for the model equation, 90th percentile confidence interval (CI), and 90th percentile prediction interval (PI) for the linear equation relating NDVI and ET*.

Equation	**β_0**	**β_1**
Linear (model)	-0.035	1.1097
Lower 90% CI band	-0.0477	1.0544
Upper 90% CI band	-0.0223	1.165
Lower 90% PI band	-0.172	1.0936
Upper 90% PI band	0.102	1.1258

The BMM approach has been successfully applied throughout the state of Nevada. Most notably, a variant of the model was used in the Humboldt River Basin. At the time of this publication, these calculations of ETg are being used in USGS modeling groundwater and surface water interactions (Huntington et al., 2022).

Actual Evapotranspiration

Estimates of actual evaporation were produced for the study area for the entire 1995-2021 study period. These data were produced as part of the tabular summaries of annual PAGD acreages, ETg rates, and ETg volume. The ETa values were calculated as defined in equations 4 and 5 from Beamer et al. (2013) and Minor (2019) as follows:

$$ETa = ETg + PPT \qquad (6).$$

Shallow Water Evaporation

Delineation

The Las Vegas Wash has undergone significant changes during the 1995-2021 study period. During this time, the channel of the Wash has been altered and restrained with the construction of weirs. Because of the dynamic nature of the Wash during the study period, a year-specific approach was essential for accurately characterizing the Wash.

A review of water-sensitive indices calculated using Landsat multispectral data (*Landsat 8*, n.d.) was conducted using Climate Engine (Huntington et al., 2017). The use of Climate Engine's graphic user interface and streamlined access to Google Earth Engine (Gorelick et al., 2017) allowed for the rapid development of methodology to discriminate shallow surface water from bare soil and vegetated land cover. Four indices were calculated and compared against corresponding aerial images to determine the best performing approach (Gao, 1996; Hall et al., 1995; McFeeters, 1996; Xu, 2006). A Modified Normalized Difference Water Index (MNDWI) as defined by Xu (2006), using Shortwave Infrared (SWIR) band 1 (1.55 – 1.75 μm) of the Landsat 8 and 9 Operational Land Imager (OLI) and equivalent bands in Landsat 5 and 7, was determined to be the best indicator of shallow surface water in the Las Vegas Wash:

$$MNDWI = \frac{Green - SWIR\ 1}{Green + SWIR\ 1} \qquad (7).$$

Google Earth Engine was used to calculate MNDWI for all available Landsat images per year, which were subsequently used to develop annual median MNDWI images (Figures 6 and 7). An approach of calculating a median value was necessary to reduce potential over- and underestimation of the spatial extents of water associated with annual variations in flow volume.

After completing a threshold analysis comparing annual median MNDWI with corresponding aerial imagery, a median MNDWI of greater than 0.03 was used to create a binary mask to indicate the presence of shallow surface water. This threshold was developed using 2020 imagery and remote sensing data. The result of the delineation was a year-specific mask of shallow water extent, which was applied to: 1) calculate rates and volumes of shallow water evaporation and 2) remove pixels from consideration of the BMM approach to develop ETg estimates. Removing pixels classified as water

Figure 6. True-color aerial image of a segment of the Las Vegas Wash, where the presence of surface water is evident.

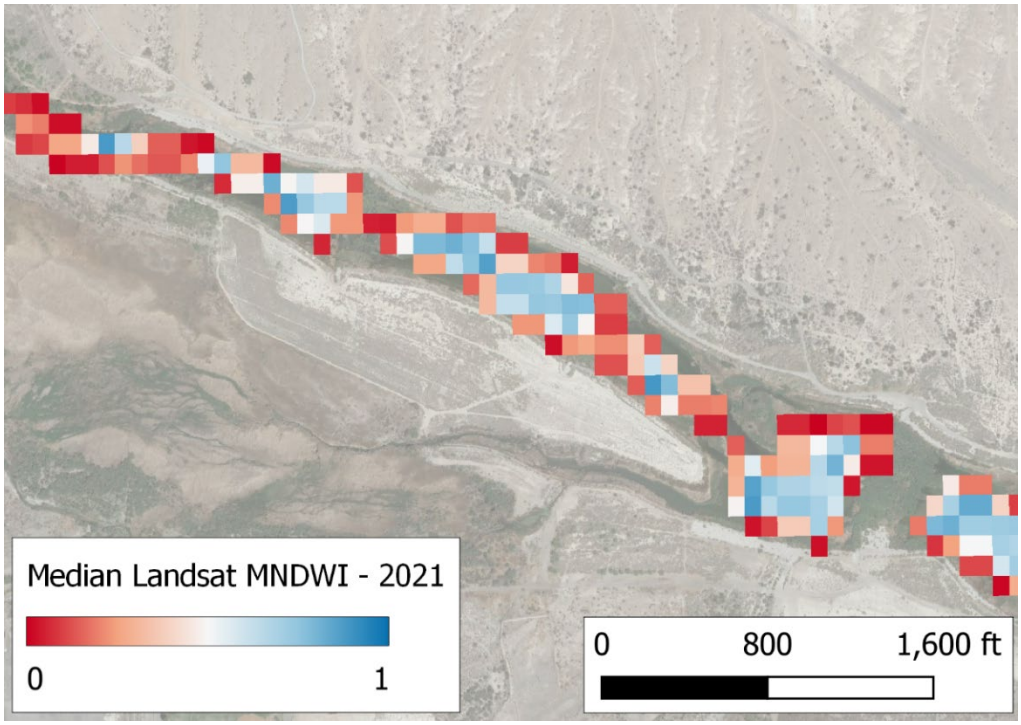

Figure 7. False-color image of MNDWI at 30-meter resolution with negative values masked superimposed on true-color aerial imagery (contrast adjusted). MNDWI values closer to 1 indicate the presence of water within the pixel area.

from the delineated potential areas of groundwater discharge was essential to prevent double-counting areas, which would lead to a systematic overestimation of volumes of water leaving the study area through ETg and evaporation.

This water classification approach was confined to the maximum extent of the delineated potential area of groundwater discharge for the entire 1995-2021 study period to exclude areas exhibiting erroneous indications of shallow water (such as the rooftops of industrial buildings) or areas not under consideration (such as residential pools and the City of Henderson Water Treatment Plant). At the request of the stakeholder, the adjacent Henderson Bird Viewing Preserve was included in estimations of evaporation for shallow surface water.

Surface water delineation for the 1995-2021 period was conducted using the previously described approach using MNDWI calculated using Landsat imagery. The Landsat data collection is natively processed and stored at the 30-meter scale. While this scale is useful for analyzing patterns and trends in landcover and vegetation, the spatial resolution results in mixed pixel effects that are especially problematic when examining narrow, linear features such as the Las Vegas Wash. Using this approach, surface water was not detectable during the years of 1995 through 1999. This period was representative of conditions prior to the construction of weirs, when the Las Vegas Wash was significantly more channelized, which resulted in a linear feature that was difficult to characterize using Landsat optical imagery acquired at 30-meter resolution. Rather than assume zero surface water evaporation, the extent was digitized based on two aerial images acquired during 1999 (Figure 8). Calculated rates and volumes of shallow water evaporation were developed using this manually delineated extent and the year specific ETo rates.

For 2000 to 2021, the MNDWI-based extent was removed from the delineated area representing annual PAGD, but the manually delineated extent could not be represented at a 30-meter resolution. Therefore, the 1995-1999 surface water extents could not be removed from the corresponding annual PAGD. Partitioning of rates and volumes of ETg and surface water evaporation at a sub-30-meter pixel resolution was beyond the scope of this project, but future work could focus on downscaling these calculations to a finer spatial scale. When this factor is considered along with the non-year-specific nature of the 1995-1999 extent of surface water in the Las Vegas Wash, it was deemed appropriate to highlight the incongruence with the surface water extents purely derived from Landsat data.

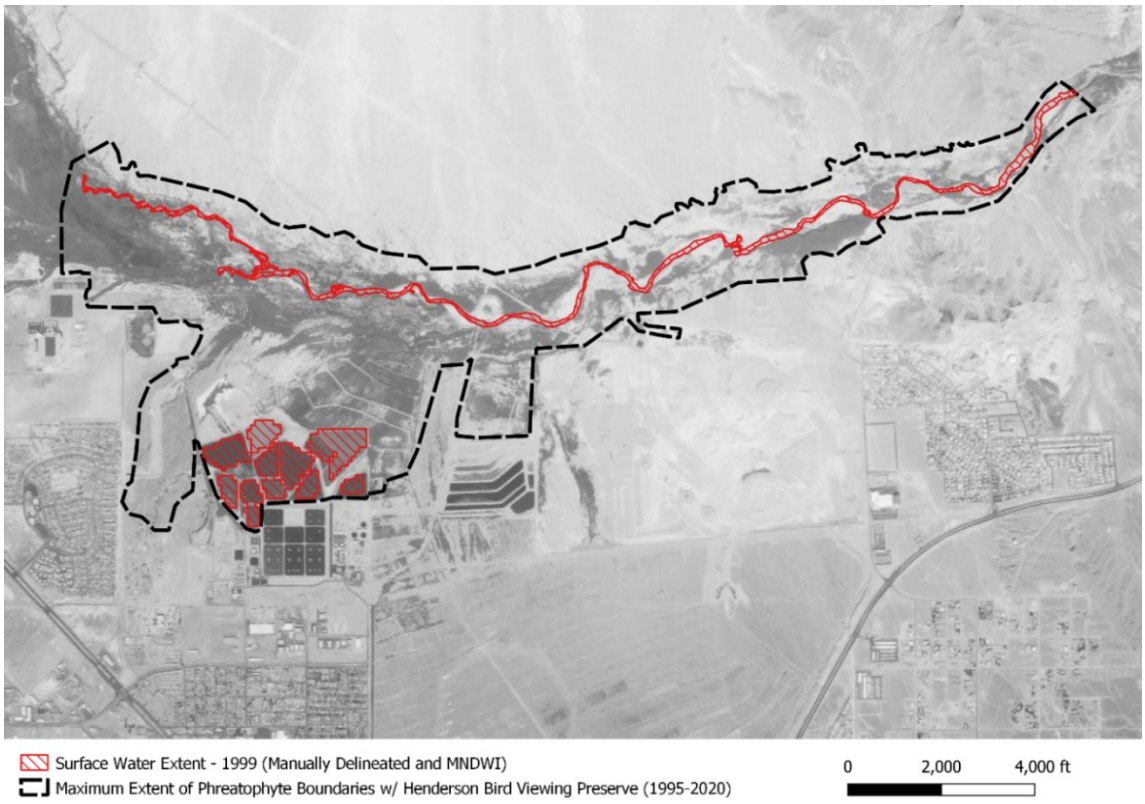

Figure 8. Surface water extent for the year 1999 developed using MNDWI approach and manual digitizing based on aerial imagery acquired in 1999.

Evaporation for the Las Vegas Wash was calculated using the approach defined by the Food and Agriculture Organization (FAO) of the United Nations in *Irrigation and Drainage Paper 56* (Allen et al., 1998). This approach was defined for open water bodies of less than two-meters in depth and calculate as:

$$E = ET_o \times 1.05 \qquad (8)$$

where E is the annual rate of evaporation and ETo is annual total grass reference ET (i.e., evaporative demand) (mm/yr). The ETo was multiplied by a factor of 1.05 to arrive at an annual rate of evaporation. This annual rate was multiplied by the surface area of the year-specific delineated surface water extent described previously in this report to arrive at a volume of shallow water evaporation.

RESULTS AND DISCUSSION

The analysis summarized in this report has indicated a decrease in the spatial extent of PAGD and ETg rates, which corresponds with an overall decrease in the volumes of ETg (Figure 9a). A comparison was made between the ETg volumes calculated in this study and the estimates of ETg reported by Ramboll in the Phase 6 study (Figure 9b). For the year 2014 this study reported a range of likely ETg values between 1,464.6 and 1,838.5 ac-ft/yr, which

(a)

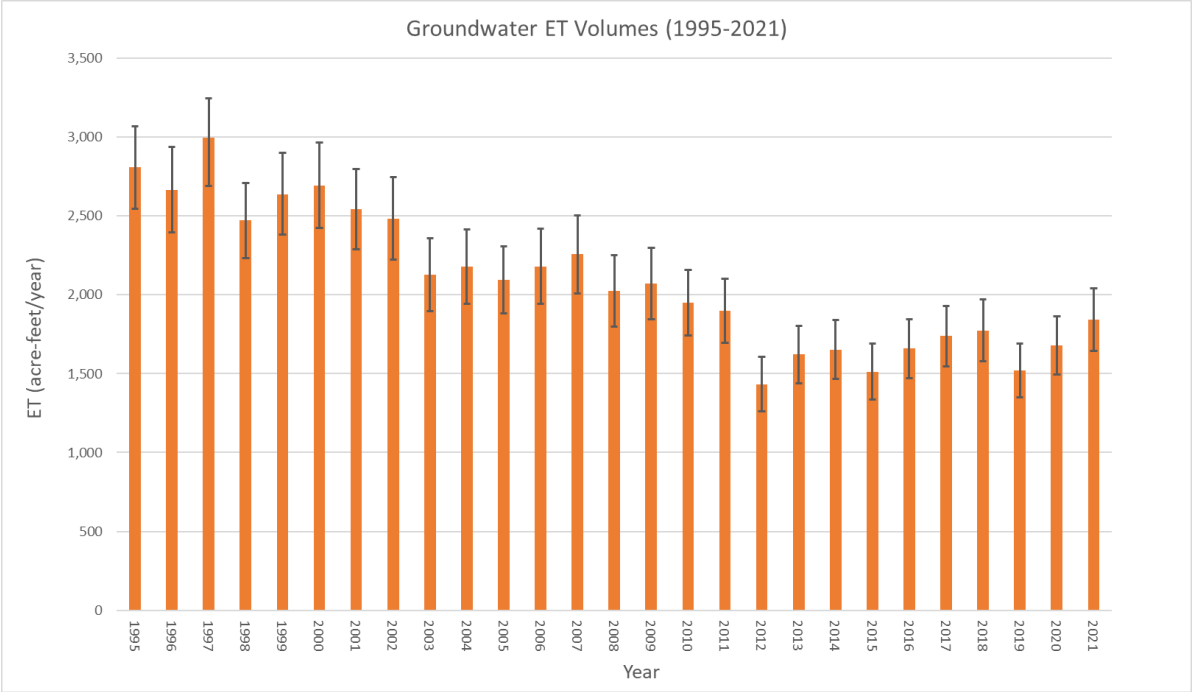

(b)

Figure 9. (a) Groundwater ET volumes for the study area for the period of 1995 to 2021. Error bars indicate the bounds of the upper and lower confidence interval. (b) Comparison between the ETg volumes calculated in this study and ETg estimates reported by Ramboll in the Phase 6 study.

is comparable to the 1,848.8 ac-ft/yr reported in the Phase 6 modelling effort. Years 2015 to 2018 show estimates in a similar magnitude, however the estimates diverge most dramatically in 2017 and 2018, when ETg volumes calculated by Ramboll are ~200 ac-ft/yr less than the lower bounds of the DRI estimates. Comparisons of ETg volumes are documented in Table 3. It is worth highlighting that the results described in this work are neither consistently higher nor lower than the estimates published in the Phase 6 model. These discrepancies in the results are potentially explained in the use of both annual and sub-annual data to develop estimates of ET and surface water evaporation. These data inputs serve to depict annual variability in landcover, vegetation conditions, and the atmospheric demand for water.

Figure 10 illustrates trends in ETa during the study period. Because ETa is calculated as ETg + PPT, ETg and ETa should appear similar over time, but they may diverge based on the magnitude of annual precipitation events. This methodology assumes that nearly all precipitation can be considered effective, whereas all precipitation is consumed through the processes of evaporation and transpiration and is not lost to runoff or groundwater percolation.

Table 3. ETg volumes reported in this study, with calculated volumes at the upper and lower 90th percentile confidence intervals (CI), compared to volumes of ETg reported in the Ramboll Phase 6 study.

Year	ETg volume (acre-ft/yr)	ETg 90% LCI (acre-ft/yr)	ETg 90% UCI (acre-ft/yr)	Ramboll-Phase 6 ETg volume (acre-ft/yr)
2014	1,651.2	1,464.6	1,838.5	1,848.8
2015	1,512.5	1,336.1	1,689.1	1,344.6
2016	1,658.1	1,473.1	1,843.3	1,525.4
2017	1,738.7	1,547.0	1,930.7	1,344.6
2018	1,773.9	1,578.1	1,969.8	1,344.6

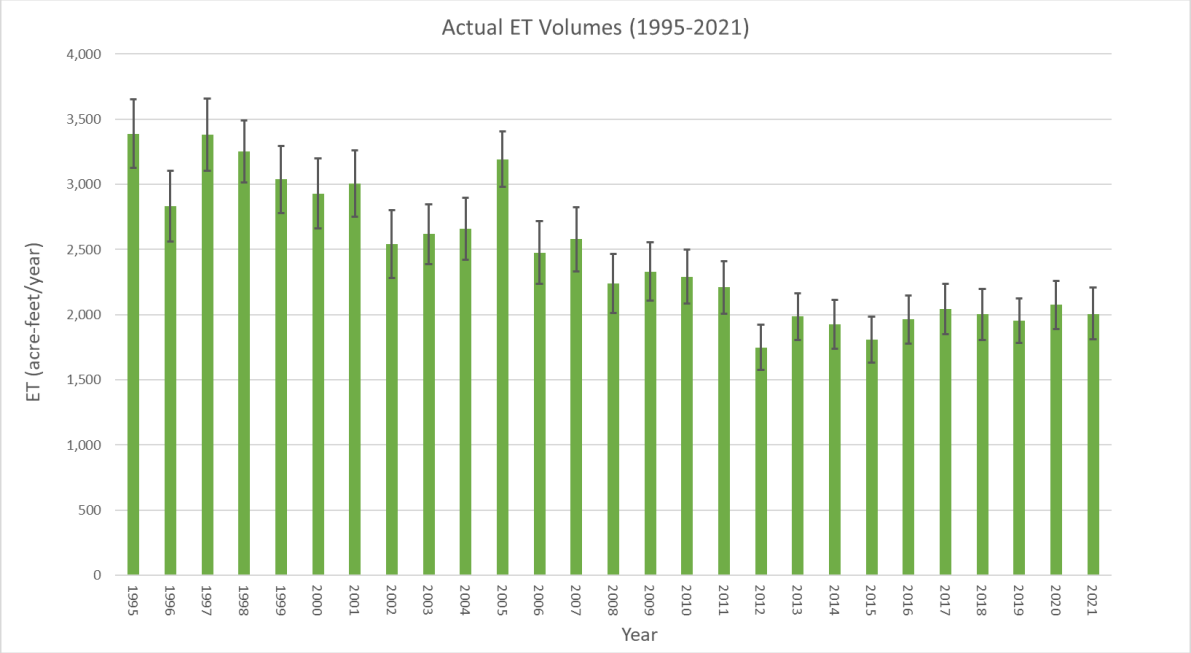

Figure 10. Actual ET volumes for the study area for the period of 1995 to 2021. Error bars indicate the bounds of the upper and lower confidence interval.

Surface water evaporation (Figure 11) depicts a downward trend in overall volumes of evaporation from 1995 to 2011, but this reduction is followed by a dramatic increase in 2012. This reversal in the reduction in evaporation coincided with the installation of weirs within the Las Vegas Wash channel. These weirs were constructed to decrease the flow velocity, thereby reducing erosion and allowing for wetlands to be established along the Wash (Burke, 2015). Because the channel of the Las Vegas Wash exists within the delineated PAGD, any increase to surface water extent resulted in an equivalent reduction in the delineated PAGD. Because volumetric calculations of ETg, ET, and evaporation are highly sensitive to the calculated area, this interplay between discharge area and surface water extent is likely a contributing factor to the decreased ETg and ETa in 2012 and following years.

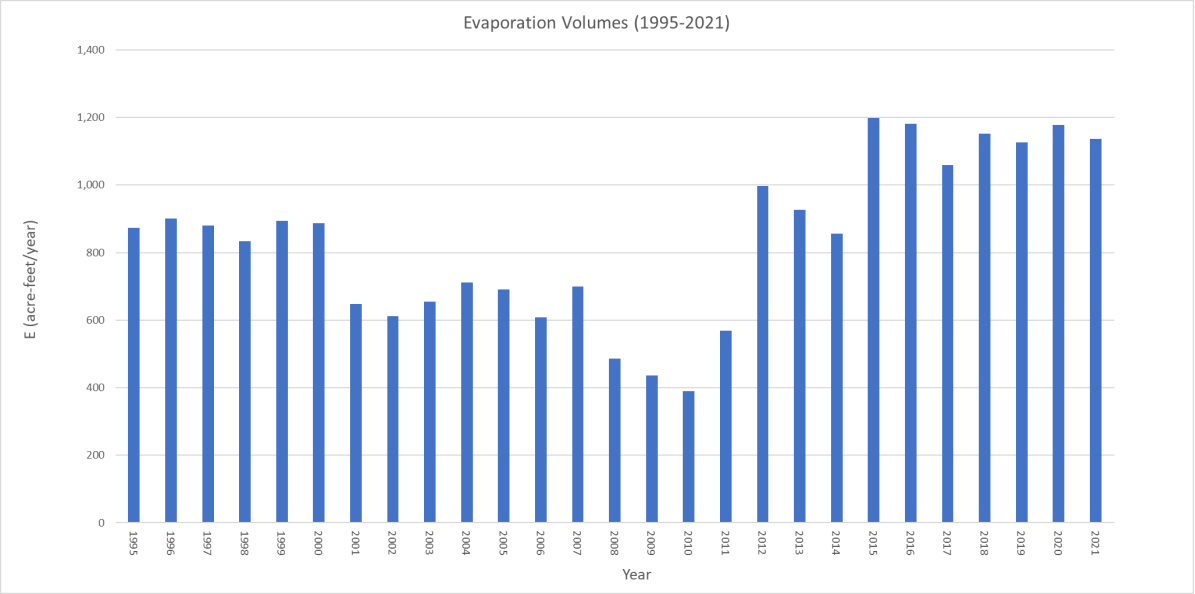

Figure 11. Evaporation volumes for the study area for the period of 1995 to 2021.

The remote sensing approach used in this study is well suited for studying large geographic areas over long time periods because the Landsat family of satellites has collected images for most locations at a frequency of one image per 16 days when one satellite has been in operation or every 8 days when two satellites have been in operation (*Landsat 8*, n.d.). The Landsat program has been in continuous operation from 1984 to the present time and is planned to continue as additional Landsat satellites are put into operation. The data collection frequency and overall duration is especially valuable for studying landscapes undergoing significant changes over long timescales. The results of this report are provided in a data package and summarized in the report appendix. Figure 12 provides an example of the spatially explicit, year-specific data developed in this study.

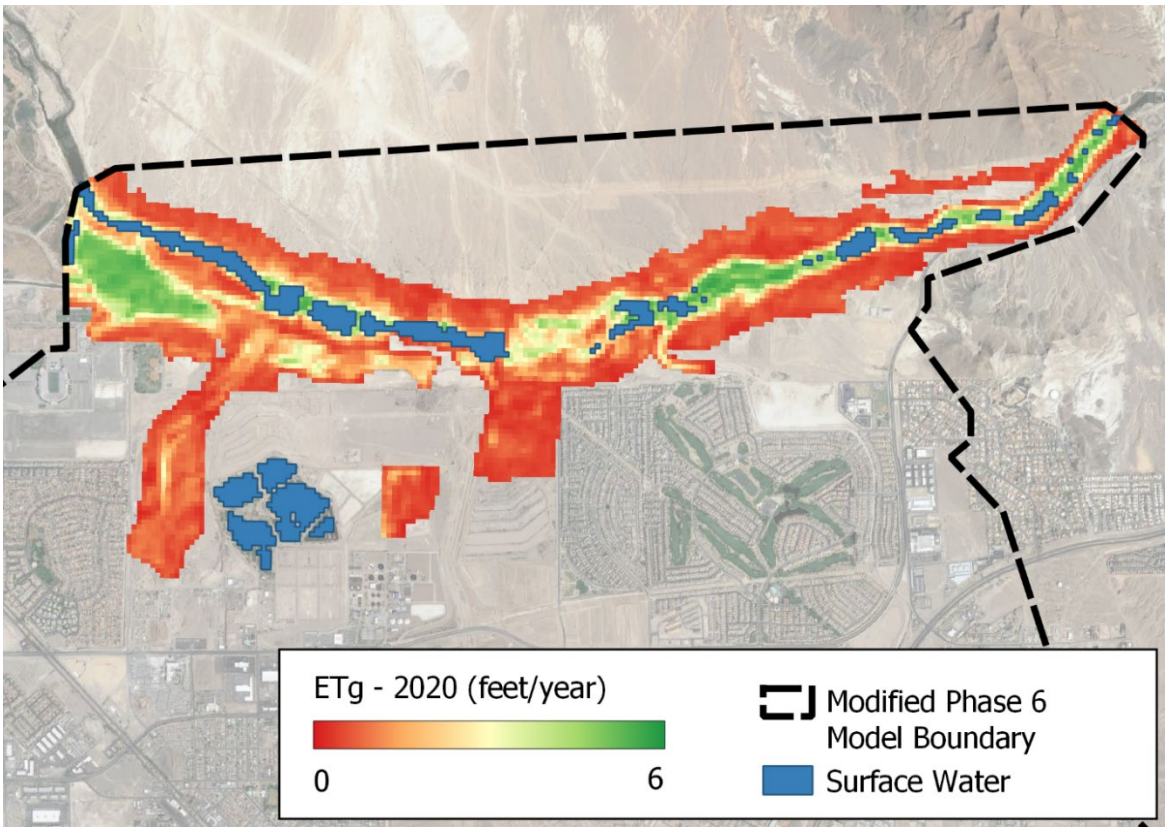

Figure 12. Example of year-specific data representing ETg rates and surface water extent.

While the annual winter precipitation is natively accounted for by the BMM, the monsoonal pattern of late-summer precipitation received by the Las Vegas area was considered as a potential source of disproportionate influence on the final data product. While precipitation is removed during the application of BMM, the influence of short bursts of precipitation and the corresponding responses in vegetation vigor were thought to be a potential issue. A comparison of ETg to the yearly sums of precipitation provided by GridMET for the ordinal days of 152 through 258 was conducted. Wet monsoonal years were identified as years when the summer received more than 1.25 inches of precipitation, which served to identify the years of 1997 to 1999 and 2012 to 2013 as especially wet. Dry monsoonal years were identified as years when the summer received less than 0.33 inches of precipitation. Dry years were identified as 2000 to 2002, 2008 to 2010, and 2019 to 2020. A time series analysis of annual rates of ETg did not reveal any obvious connections between summer precipitation and calculations of ETg (Figure 13). Additional analysis of ETg and PPT revealed a calculated R-squared value of near zero, indicating that precipitation events between days 152-258 likely did not explain variations in calculated ETg. Therefore, it is assumed that subtracting annual PPT in the BMM workflow was adequate for removing the influence of monsoonal precipitation from the calculations of ETg.

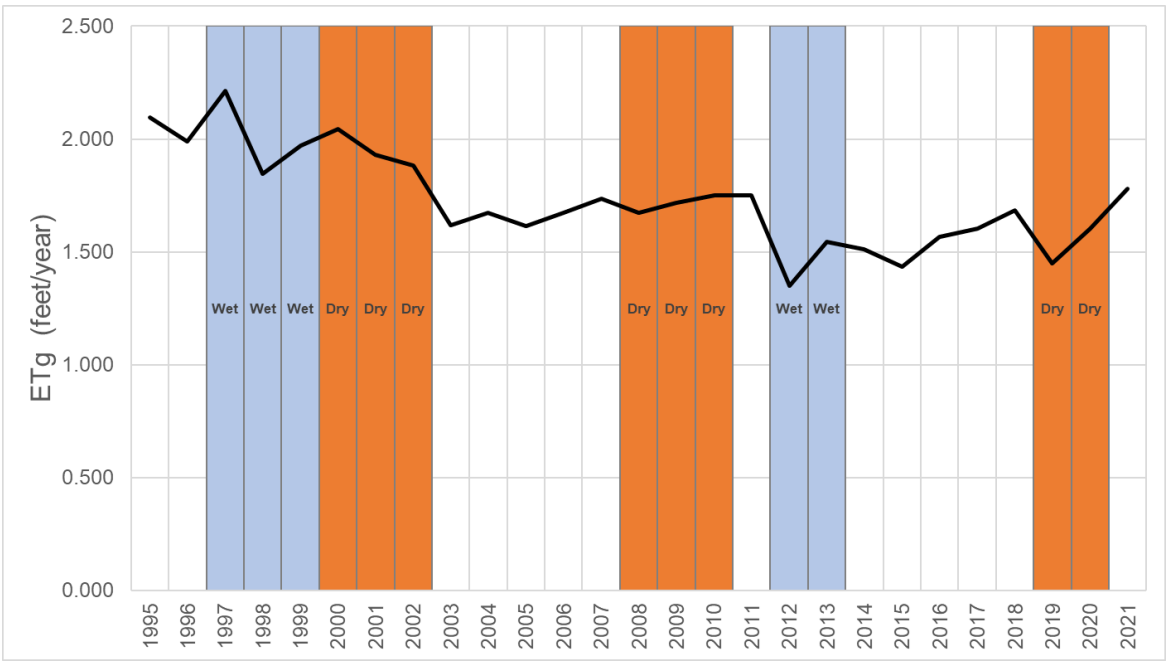

Figure 13. ETg rates compared to precipitation totals from the day of year 152 through 258. Highlighted "wet" years were defined as summers that received greater than 1.25 in of precipitation and "dry" years were defined as having less than 0.33 in of precipitation.

Upon the completion of this report the spatially explicit rates of ETg and ET will likely require some post-processing to be integrated into the Phase 7 modelling effort. This postprocessing will likely entail generalizing the spatial component of the data into averaged rates of ET. While the resampled data will no longer exhibit the same spatial variability present in the original data, it will undoubtedly benefit from the underlying accuracy of the spatially and temporally explicit inputs of the model that were used to produce the data.

LIMITATIONS

The estimates of ETg in this report are subject to numerous limitations and uncertainties. These limitations and uncertainties include 1) the empirical data and models used in the study, 2) the climate datasets used in the application of the models, 3) the accuracy of the calibrations used in developing Landsat at-surface reflectance and the degree to which derived indices accurately represent vegetation vigor and the presence of water, and 4) the accuracy of year-specific delineated areas of potential groundwater discharge. The empirical NDVI – ET* model is based on 54 site years of in situ ET estimates derived from advanced micrometeorological methods, which have been characterized as having +/-10 to 12 percent uncertainty (Maurer et al., 2005; Moreo et al., 2007; Allander et al., 2009). The NDVI – ET* model also assumes that all the annual precipitation is consumed by ET (i.e., no runoff) in the estimates of ETg. Although this assumption is common when estimating ETg from hydrologically closed groundwater discharge areas in the Great Basin, it may lead to an overestimation of ETg in areas where substantial runoff occurs.

The gridMET ETo was evaluated for accuracy by comparing gridMET monthly ETo to monthly ETo calculated from data collected at representative weather stations near the study area. The results for all sites indicated that annual gridMET calculations of ETo were within 5 percent, but annual individual station biases were calculated as -14 percent, 5 percent, and 25 percent (Table 2). Given the lack of consistent bias, it was decided that gridMET ETo would be used in its native format. Previous studies in Nevada that have compared gridMET precipitation to station data have suggested that gridMET is reasonably accurate. These comparisons are potentially problematic because station measurements of PPT represent unknown certainty (McEvoy et al., 2014; McEvoy and McCurdy, 2018). Additional research may be useful in further characterizing potential gridMET biases.

The BMM approach used in this study relies on Landsat at-surface reflectance data products and recently standardized atmospheric correction procedures developed by the USGS (USGS, 2022). Aerosols, clouds, haze, and water vapor are all factors known to affect atmospheric correction and the approach used in this study leverages state-of-the-art weather model outputs and ancillary satellite data to address these complexities. The QA/QC-ed Landsat images used in this study to compute NDVI, ET*, and ETg were acquired from the June 1st to September 15th (day of year 152 through 258, non-leap year) period. Single estimates of these variables were derived for each year of the study period to characterize the phreatophyte vegetation vigor and ETg. Although the use of single or composite values may not adequately characterize conditions for the entire year, multiple studies have demonstrated the usefulness of single and composite satellite-based ET approaches for estimating ETa and ETg from areas of potential groundwater discharge (Groeneveld et al., 2007; Beamer et al., 2013; Minor, 2019) and that these estimates compare well to riparian ET estimates based on advanced surface energy balance (SEB) and time integration models that require iterative processing (Khand et al., 2017). Challenges in accurately estimating ET in arid environments with relatively low to moderate vegetation cover using SEB and time integration methods (e.g., Allen et al. [2007]) are centered around: 1) the need to accurately account for PPT and subsequent ET events that occur before or after image acquisitions, ideally using daily soil water balance models (which have their own set of uncertainties and application challenges); and 2) the fact that estimates of net radiation and sensible heat flux are both large quantities in areas of low ET. Because ET is solved as a residual of the energy balance, this leads to errors in ET that may exceed the actual ET (i.e., differencing two large numbers, net radiation, and sensible heat flux to solve for ET). This can be a problem when estimating annual ETg (annual ETa less annual PPT) from phreatophyte shrublands where annual ETg is typically a small fraction of annual ETa. An empirical single or seasonal composite approach that is based on in situ measurements of annual ETa and gridded estimates of PPT and ETo, such as applied in this study, constrains annual ETg estimates to in situ measurements of ETa and ETg. This approach avoids challenges and associated errors with time integration between image dates and can provide an estimate of uncertainty based on confidence intervals around the mean of least-squares regression models.

Given the many assumptions and complexities of estimating and scaling ETg rates from flux towers to the basin scale, relying on the NDVI – ET* regression model used in this study (or a similar approach) is attractive because it is based on 54 site years of in situ ET estimates and Landsat vegetation indices for phreatophyte areas in the Great Basin. This approach also accounts for temporal and spatial variations in evaporative demand and

precipitation, which are two main drivers of ET. When all these factors and limitations are considered, single-scene or composite approaches are more robust and likely more accurate than advanced SEB models or simple ET Unit approaches in which previous study ET rates are assumed to be constant in time and space and are applied across similar ET Units for the study areas of interest. The NDVI – ET* approach used in this study overcomes multiple challenges in estimating long-term ETg for groundwater discharge areas, but it does have limitations that are common with empirical regression models in addition to limited accuracy for estimating low rates of ETg in areas of sparse vegetation. These limitations are most evident in the inherent issues of low signal to noise and uncertainty in bare soil contributions to ETg.

A significant source of uncertainty in estimating ETg volumes is the delineation of potential areas of groundwater discharge (Zhu and Young, 2009). Potential areas of groundwater discharge were based on a combination of aerial imagery, multispectral satellite imagery (including thermal data), records of depth to groundwater, GIS datasets of topography, vegetation, and phreatophyte delineations from previous studies. Field investigations were initially proposed as an optional effort, but they were deemed to be unnecessary because there was a high degree of confidence in the accuracy of PAGD representing near-present conditions. Conditions in previous decades were likely less precise because the delineation of historical discharge boundaries was limited by the representative data available, particularly the availability of high-resolution aerial imagery. Although actual areas of groundwater discharge may be smaller than the potential areas delineated in this study, areas of minimal ETg typically exhibit exceptionally low NDVI values, and therefore the predicted ETg for these areas will be negligible using the BMM approach.

Estimates of volumes of surface water evaporation are similarly affected by uncertainties in the delineation of areas of surface water. As this work relies on Landsat data processed at 30-meter resolution, it was beneficial to delineate the areas of surface water at the same spatial scale. While larger areas of water near the constructed weirs were straightforward in characterization using the MNDWI-based approach, narrow, channelized areas of surface water were difficult to discern using Landsat-resolution data. Due to the limitation in spatial resolution of the remote sensing data, it is likely that many mixed-pixels containing both vegetation and surface water were classified as vegetation in this workflow due to the spectral signature exhibited by the individual pixels. This underestimation of water leaving the Wash system through evaporation is likely offset in part by overestimates of water leaving the system via ETg from riparian vegetation adjacent to the Wash, which benefits from enhanced access to water.

CONCLUSION

ET data were produced for the specific use of improving modeling for groundwater flow and contaminate transport for the study area as part of the larger effort of management and remediation at the NERT site by the Nevada Department of Environmental Protection (NDEP). The data corresponding to this report summarizes rates and volumes of ETg, ETa, and shallow surface water evaporation for the 1995-2021 study period. The ETg data were provided in raster and tabular formats and aggregated to the NERT Phase 7 modeling units. The ETa and evaporation data are summarized at the annual time step in tabular form.

Calculated volumes of ETg for the study area were initially 2,807 acre-feet/year for 1995 but decreased to 1,872 acre-feet/year by 2021. This reduction in ETg is most attributable to a reduction in the overall spatial extent of the potential areas of groundwater discharge.

This work improves upon the techniques employed in the previous modeling efforts in The Las Vegas Wash and adjacent properties as the Phase 6 model assumed a maximum fixed rate of 5.11 ft/yr of ETg across the entire delineated area of phreatophytic vegetation (Ramboll, 2019). Given the dynamic nature of the Las Vegas Wash and the surrounding area, a spatially explicit, year-specific approach was essential to account for variations in phreatophyte extent, vegetation vitality, shallow water extent, and annual reference ET. The inherent accuracy of these data would not be compromised if appropriate methods are used to integrate the data into the Phase 7 model, such as converting the data into a spatially averaged rate for a single timestep.

The primary method used in this study was developed specifically from the analysis of phreatophytic vegetation in Nevada and the Great Basin and it has been applied throughout the region. Landsat data processed using Google Earth Engine provides high-quality, spatially explicit, year-specific estimates of ETa, ETg, and shallow water evaporation. This approach uses the latest and most-accurate version of Landsat data and leverages the 35-plus years of optical and thermal data acquired by the Landsat series of satellites. This overarching effort made use of cloud computing, logs of depth to groundwater from local wells, year-specific GIS data, historical data pertaining to phreatophytic vegetation, and empirical regression models based on ET data collected in areas of phreatophyte vegetation.

REFERENCES

Abatzoglou, J. T. (2013). Development of gridded surface meteorological data for ecological applications and modelling. *International Journal of Climatology*, *33*(1), 121-131.

Allander, K. K., Smith, J. L., & Johnson, M. J. (2009). *Evapotranspiration from the Lower Walker River Basin, West-Central Nevada, Water Years 2005-07*: U.S. Geological Survey Scientific Investigations Report 2009-5079, 62 p. Retrieved May 6, 2015, from http://pubs.usgs.gov/sir/2009/5079/

Allen, R. G. (1996). Assessing integrity of weather data for reference evapotranspiration estimation. Journal of irrigation and drainage engineering, 122(2), 97-106.

Allen, R. G., Walter, I. A., Elliot, R., & Howell, T. A. (2005). ASCE-EWRI Standardization of Reference Evapotranspiration. *American Society of Civil Engineers–Environmental Water Institute*.

Allen, R. G., Tasumi, M., & Trezza, R. (2007). *Satellite-Based Energy Balance for Mapping Evapotranspiration with Internalized Calibration (METRIC)* – Model. Journal of Irrigation and Drainage Engineering, 133(4): 380-394. doi:10.1061/(ASCE)0733-9437(2007)133:4(380).

Arnone, J., Jasoni, R., Fenstermaker, L., Wolfahrt, G., Kraftt, C., Lyles, B., Healey, J., Young, M., & Thomas, J. (2008). *Variable evapotranspiration water losses from lowland agricultural and native shrubland ecosystems in the Great Basin of Nevada.* (DRI Publication 655.7520).

Beamer, J. P., Huntington, J. L., Morton, C. G., & Pohll, G. M. (2013). Estimating Annual Groundwater Evapotranspiration from Phreatophytes in the Great Basin Using Landsat and Flux Tower Measurements. *JAWRA Journal of the American Water Resources Association*, *49*(3), 518-533. https://doi.org/10.1111/jawr.12058

Berger, D. L., Mayers, C. J., Garcia, C. A., Buto, S. G., & Huntington, J. M. (2016). *Budgets and chemical characterization of groundwater for the Diamond Valley flow system, central Nevada, 2011-12* (USGS Numbered Series No. 2016-5055; Scientific Investigations Report). U.S. Geological Survey. https://doi.org/10.3133/sir20165055

Burke, M. (2015). RESTORATION OF THE LAS VEGAS WASH AND ASSOCIATED WETLANDS IN LAS VEGAS, NEVADA. Hydrology and Water Resources in Arizona and the Southwest. https://repository.arizona.edu/handle/10150/621704

DeMeo, G. A., Smith, J. L., Damar, N. A., & Darnell, J. (2008). *Quantifying Ground-Water and Surface-Water Discharge from Evapotranspiration Processes in 12 Hydrographic Areas of the Colorado Regional Ground-Water Flow System, Nevada, Utah, and Arizona* (Scientific Investigations Report No. 2008-5116; p. 36). https://pubs.usgs.gov/sir/2008/5116/

DeMeo, G. A. (2018). *Evapotranspiration data from two sites at the head of the East Walker River near Bridgeport, CA, June 2012 through September 2013* [Data set]. U.S. Geological Survey. https://doi.org/10.5066/F79C6WM9

Gao, B. (1996). NDWI—A normalized difference water index for remote sensing of vegetation liquid water from space. *Remote Sensing of Environment*, *58*(3), 257-266. https://doi.org/10.1016/S0034-4257(96)00067-3

Garcia, C. A., Huntington, J. M., Buto, S. G., Moreo, M. T., Smith, J. L., & Andraski, B. J. (2014). *Groundwater discharge by evapotranspiration, Dixie Valley, west-central Nevada, March 2009-September 2011* (USGS Numbered Series No. 1805; Professional Paper, p. 104). U.S. Geological Survey. https://doi.org/10.3133/pp1805

Gorelick, N., Hancher, M., Dixon, M., Ilyushchenko, S., Thau, D. & Moore, R. (2017). Google Earth Engine: Planetary-scale geospatial analysis for everyone. Remote Sensing of Environment, 202(1), 18-27. https://doi.org/10.1016/j.rse.2017.06.031

Groeneveld, D., Baugh, W., Sanderson, J., & Cooper, D. (2007). Annual Groundwater Evapotranspiration Mapped from Single Satellite Scenes. *Journal of Hydrology - J HYDROL*, *344*, 146-156. https://doi.org/10.1016/j.jhydrol.2007.07.002

Hall, F. G., Townshend, J. R., & Engman, E. T. (1995). Status of remote sensing algorithms for estimation of land surface state parameters. *Remote Sensing of Environment*, *51*(1), 138-156. https://doi.org/10.1016/0034-4257(94)00071-T

Harrill, J. R. (1976). Pumping and Ground-Water Storage Depletion in Las Vegas Valley, Nevada, 1955-1974: Nevada Department of Conservation and Natural Resources, Department of Water Resources, Water Resources Bulletin 44, pl. 1.

Harrill, J. R., Gates, J. S., & Thomas, J. M. (1988). Major ground-water flow systems in the Great Basin region of Nevada, Utah, and adjacent States: U.S. Geological Survey Hydrologic Investigations Atlas HA-694-C, scale 1:1,000,000, 2 sheets.

Huntington, J. L., McGwire, K. C., Morton, C. G., Snyder, K., Peterson, S., Erickson, T., Niswonger, R., Carroll, R. W., Smith, G. T., Allen, R. (2016). Assessing the Role of Climate and Resource Management on Groundwater Dependent Ecosystem Changes in Arid Environments with the Landsat Archive, Remote Sensing of Environment, 185, 186-197, 10.1016/j.rse.2016.07.004

Huntington, J. L., Hegewisch, K. C., Daudert, B., Morton, C. G., Abatzoglou, J. T., McEvoy, D. J., & Erickson, T. (2017). Climate Engine: Cloud Computing and Visualization of Climate and Remote Sensing Data for Advanced Natural Resource Monitoring and Process Understanding. *Bulletin of the American Meteorological Society*, *98*(11), 2397-2410. https://doi.org/10.1175/BAMS-D-15-00324.1

Huntington, J., Bromley, M., Minor, B., Morton, C., & Smith, G. (2022). *Groundwater Discharge from Phreatophyte Vegetation, Humboldt River Basin, Nevada* (Publication No. 41288). Division of Hydrologic Sciences, Desert Research Institute. https://www.dri.edu/project/humboldt-etg/

Khand, K., Taghvaeian, S., & Hassan-Esfahani, L. (2017). *Mapping Annual Riparian Water Use Based on the Single-Satellite-Scene Approach*. Remote Sensing, 9(8), 832.

Landsat 8. (n.d.). Retrieved May 13, 2015, from http://landsat.usgs.gov/landsat8.php

Landsat 8-9 Collection 2 Level 2 Science Product Guide | U.S. Geological Survey. (2022). https://www.usgs.gov/media/files/landsat-8-9-collection-2-level-2-science-product-guide

Leuning, R., Gorsela, E. van, Massman, W. J., & Isaac, P. R. (2012). Reflections on the surface energy imbalance problem. *Agricultural and Forest Meteorology. 156: 65-74.*, 65-74. https://doi.org/10.1016/j.agrformet.2011.12.002

Malmberg, G. T. (1965). Available water supply of the Las Vegas ground-water basin, Nevada: U.S. Geological Survey Water-Supply Paper 1780, 116 p.

Maurer, D. K., Berger, D. L., Tumbusch, M. L., & Johnson, M. J. (2005). *Rates of Evapotranspiration, Recharge from Precipitation Beneath Selected Areas of Native Vegetation, and Streamflow Gain and Loss in Carson Valley, Douglas County, Nevada, and Alpine County, California* (Scientific Investigations Report No. 2005-5288; p. 70). USGS. https://pubs.usgs.gov/sir/2005/5288/

Maxey, G. B. & Jameson, C. H. (1948). Geology and water resources of Las Vegas, Pahrump, and Indian Spring Valley, Clark and Nye Counties, Nevada: Nevada State Engineer, Water Resources Bulletin 5, pl. 7.

McEvoy, D. J., Mejia, J. F., & Huntington, J. L. (2014). *Use of an observation network in the Great Basin to evaluate gridded climate data*. Journal of Hydrometeorology, 15(5), 1913- 1931.

McEvoy, D. J., and McCurdy, G. (2018). *Washoe County Rain Gauge Network: Historical Analysis and Comparison to PRISM*. Desert Research Institute Report prepared for Western Regional Water Commission, 27 pp.

McFeeters, S. K. (1996). The use of the Normalized Difference Water Index (NDWI) in the delineation of open water features. *International Journal of Remote Sensing*, *17*(7), 1425-1432. https://doi.org/10.1080/01431169608948714

McGwire, K., Minor, T., & Fenstermaker, L. (2000). Hyperspectral Mixture Modeling for Quantifying Sparse Vegetation Cover in Arid Environments. *Remote Sensing of Environment*, *72*(3), 360-374. https://doi.org/10.1016/S0034-4257(99)00112-1

Minor, B. (2019). *Estimating Annual Groundwater Evapotranspiration from Hydrographic Areas in the Great Basin using Remote Sensing and Evapotranspiration Data Measured by Flux Tower Systems* [unpublished master's thesis]. University of Nevada, Reno.

Moreo, M. T., Andraski, B. J., & Garcia, C. A. (2017). *Groundwater discharge by evapotranspiration, flow of water in unsaturated soil, and stable isotope water sourcing in areas of sparse vegetation, Amargosa Desert, Nye County, Nevada* (USGS Numbered Series No. 2017-5079; Scientific Investigations Report, p. 68). U.S. Geological Survey. https://doi.org/10.3133/sir20175079

Moreo, M. T., Laczniak, R. J., & Stannard, D. I. (2007). *Evapotranspiration Rate Measurements of Vegetation Typical of Ground-Water Discharge Areas in the Basin and Range Carbonate-Rock Aquifer System, White Pine County, Nevada, and Adjacent Areas in Nevada and Utah, September 2005-August 2006* (Numbered Series No. 2007-5078; Scientific Investigations Report). USGS. https://doi.org/10.3133/sir20075078

Nichols, W. D. (1994). Groundwater discharge by phreatophyte shrubs in the Great Basin as related to depth to groundwater. Water Resources Research, 30(12), 3265-3274.

Nichols, W.D. (2000). Regional Ground-Water Evapotranspiration and Ground-Water Budgets, Great Basin, Nevada: U.S. Geological Survey Professional Paper 1628, 82 pp.

Pastorello, G., Trotta, C., Canfora, E., Chu, H., Christianson, D., Cheah, Y.-W., Poindexter, C., Chen, J., Elbashandy, A., Humphrey, M., Isaac, P., Polidori, D., Reichstein, M., Ribeca, A., van Ingen, C., Vuichard, N., Zhang, L., Amiro, B., Ammann, C., … Papale, D. (2020). The FLUXNET2015 dataset and the ONEFlux processing pipeline for eddy covariance data. *Scientific Data*, *7*(1), Article 1. https://doi.org/10.1038/s41597-020-0534-3

pyWeatherQAQC - Graphical Weather Data Correction—PyWeatherQAQC 0.3.0 documentation. (n.d.). Retrieved August 2, 2022, from https://wswup.github.io/pyWeatherQAQC/

Ramboll (2019). Phase 6 Groundwater Flow and Transport Model, Nevada Environmental Response Trust Site, Henderson, Nevada. Ramboll, Emeryville, CA.

Ramboll (2019). Annual Remedial Performance Report for Chromium and Perchlorate Nevada Environmental Response Trust Site (Former Tronox LLC Site) Henderson, Nevada. Annual Report. Emeryville, California, December 31, 2019.

Reiner, S. R., Laczniak, R. J., DeMeo, G. A., Smith, J. L., Elliot, P. E., Nylund, W. E., & Fridrich, C. J. (2002). *Ground-Water Discharge, Oasis Valley, Nevada* (WRIR No. 01-4239). USGS. https://pubs.usgs.gov/wri/wri014239/

Reiner, S.R., Laczniak, R.J., DeMeo, G.A., Smith, J.L., Elliott, P.E., Nylund, W.E., & Fridrich, C.J. (2002). Groundwater Discharge Determined from Measurements of Evapotranspiration, Other Available Hydrologic Components, and Shallow Water-Level Changes, Oasis Valley, Nye County, Nevada: U.S. Geological Survey Water-Resources Investigations Report 01-4239, 65 p. http://pubs.usgs.gov/wri/wri014239.Robinson, T.W. (1958). Phreatophytes: U.S. Geological Survey Water-Supply Paper 1423, https://pubs.usgs.gov/wsp/1423/report.pdf.

Schmidt, G., Jenkerson, C. B., Masek, J., Vermote, E., & Gao, F. (2013). *Landsat ecosystem disturbance adaptive processing system (LEDAPS) algorithm description* (USGS Numbered Series No. 2013-1057; Open-File Report, p. 27). U.S. Geological Survey. https://doi.org/10.3133/ofr20131057

Smith, J.L., Laczniak, R.J., Moreo, M.T., & Welborn, T.L. (2007). Mapping evapotranspiration units in the Basin and Range carbonate-rock aquifer system, White Pine County, Nevada, and adjacent parts of Nevada and Utah: U.S. Geological Survey Scientific Investigations Report 2007-5087, 20p.

Southern Nevada Water Authority. (n.d.). Las Vegas Wash. Retrieved March 6, 2023, from https://www.snwa.com/environment/las-vegas-wash/index.html

U.S. Geological Survey (USGS) (2022). Landsat 8 Surface Reflectance Code (LaSRC) Product, version 4.0, March 2022, 37 p.

Westenburg, C. L., DeMeo, G. A., & Tanko, D. J. (2006). *Evaporation from Lake Mead, Arizona and Nevada, 1997-99*. https://pubs.usgs.gov/sir/2006/5252/

WSWUP/gridwxcomp: Comparison of weather station and gridded climate datasets. (n.d.). Retrieved November 23, 2022, from https://github.com/WSWUP/gridwxcomp

Wu, W. (2014). The Generalized Difference Vegetation Index (GDVI) for Dryland Characterization. *Remote Sensing*, *6*(2), Article 2. https://doi.org/10.3390/rs6021211

Xu, H. (2006). Modification of normalized difference water index (NDWI) to enhance open water features in remotely sensed imagery. *International Journal of Remote Sensing*, *27*(14), 3025-3033. https://doi.org/10.1080/01431160600589179

Zachariassen, J., Zeller, K. F., Nikolov, N., & McClelland, T. (2003). A review of the Forest Service Remote Automated Weather Station (RAWS) network. *Gen. Tech. Rep. RMRS-GTR-119. Fort Collins, CO: U.S. Department of Agriculture, Forest Service, Rocky Mountain Research Station. 153 p + CD.*, *119*. https://doi.org/10.2737/RMRS-GTR-119

Zhu, J., & Young, M. H. (2009). Sensitivity and Uncertainty of Ground-Water Discharge Estimates for Semiarid Shrublands 1. JAWRA Journal of the American Water Resources Association, 45(3), 641-653. https://doi.org/10.1111/j.1752-1688.2009.00312.x

APPENDIX A. ANNUAL EVAPOTRANSPIRATION AND SURFACE WATER EVAPORATION SUMMARIES

Table A-1. Annual ET summaries 1995-2021.

Year	Area (acres)	PPT rate (ft/yr)	ETa rate (ft/yr)	ETg rate (ft/yr)	PPT volume (acre-ft/yr)	ETa volume (acre-ft/yr)	ETg volume (acre-ft/yr)	ETg 90% LCI (acre-ft/yr)	ETg 90% UCI (acre-ft/yr)
1995	1,339.3	0.43	2.53	2.10	582.5	3,389.7	2,807.5	2,545.1	3,070.1
1996	1,339.3	0.12	2.11	1.99	165.3	2,830.5	2,665.6	2,393.7	2,937.9
1997	1,339.3	0.31	2.53	2.22	415.7	3,382.2	2,996.4	2,687.7	3,245.1
1998	1,339.3	0.58	2.43	1.85	779.4	3,251.7	2,472.0	2,233.5	2,710.7
1999	1,339.3	0.30	2.27	1.97	399.7	3,038.1	2,638.2	2,380.2	2,897.7
2000	1,316.4	0.18	2.23	2.05	237.2	2,930.5	2,692.1	2,421.6	2,963.7
2001	1,316.4	0.35	2.29	1.93	466.1	3,008.0	2,541.8	2,287.9	2,796.0
2002	1,317.5	0.05	1.93	1.88	59.8	2,541.9	2,482.1	2,220.7	2,744.4
2003	1,314.4	0.37	1.99	1.62	492.9	2,619.5	2,126.2	1,897.8	2,356.2
2004	1,302.1	0.37	2.04	1.67	482.7	2,659.9	2,177.5	1,941.3	2,414.2
2005	1,296.4	0.85	2.46	1.62	1098.9	3,193.9	2,094.7	1,881.8	2,307.8
2006	1,304.6	0.23	1.90	1.67	296.0	2,476.6	2,180.6	1,942.1	2,420.0
2007	1,301.0	0.25	1.98	1.73	322.5	2,578.6	2,256.1	2,010.1	2,503.2
2008	1,209.9	0.18	1.85	1.67	213.6	2,238.4	2,024.8	1,800.3	2,250.1
2009	1,205.8	0.21	1.93	1.72	258.8	2,330.1	2,071.2	1,846.8	2,296.1
2010	1,112.9	0.31	2.06	1.75	342.8	2,291.7	1,948.9	1,742.6	2,155.4
2011	1,083.5	0.29	2.04	1.75	310.8	2,209.1	1,898.4	1,697.4	2,099.4
2012	1,060.6	0.30	1.65	1.35	314.1	1,747.2	1,433.1	1,261.5	1,606.7
2013	1,048.2	0.35	1.89	1.55	364.9	1,985.7	1,620.8	1,440.7	1,800.9
2014	1,092.6	0.25	1.76	1.51	274.8	1,926.0	1,651.2	1,464.6	1,838.5
2015	1,054.8	0.28	1.71	1.43	296.3	1,808.8	1,512.5	1,336.1	1,689.1
2016	1,058.6	0.29	1.85	1.57	304.7	1,962.8	1,658.1	1,473.1	1,843.3
2017	1,084.0	0.28	1.89	1.60	305.1	2,043.9	1,738.7	1,547.0	1,930.7
2018	1,053.9	0.22	1.90	1.68	230.3	2,004.2	1,773.9	1,578.1	1,969.8
2019	1,048.2	0.41	1.86	1.45	432.6	1,953.2	1,520.6	1,348.6	1,692.6
2020	1,047.7	0.38	1.98	1.60	396.4	2,076.3	1,679.9	1,494.3	1,865.5
2021	1,051.5	0.16	1.91	1.75	167.2	2,007.3	1,841.4	1,642.5	2,040.8

Table A-2. Annual summaries of surface water evaporation 1995-2021.

Year	Area (acres)	E rate (ft/yr)	E volume (acre-ft/yr)
1995	122 *	7.25	884.4
1996	116.4 *	7.76	903.1
1997	117.8 *	7.44	875.7
1998	120.7 *	6.91	833.7
1999	122.9 *	7.34	902.4
2000	114.1	7.64	871.1
2001	87.0	7.54	655.8
2002	78.7	7.72	608.1
2003	89.6	7.35	658.5
2004	93.9	7.44	698.5
2005	98.3	7.22	710.2
2006	80.3	7.55	606.4
2007	89.4	7.85	701.6
2008	63.2	7.70	486.6
2009	57.4	7.60	436.2
2010	51.8	7.45	385.9
2011	76.0	7.41	563.0
2012	135.8	7.43	1008.8
2013	127.4	7.17	913.4
2014	117.4	7.38	866.2
2015	164.3	7.28	1195.2
2016	160.1	7.49	1199.0
2017	143.4	7.43	1065.4
2018	149.9	7.50	1123.4
2019	157.4	7.16	1126.8
2020	156.5	7.69	1203.6
2021	148.7	7.56	1124.5

Note: The asterisk (*) denotes the use of manually digitized extents of surface water used in conjunction with MNDWI approach.

STANDING DISTRIBUTION LIST

Weiquan Dong
Professional Engineering Specialist
Nevada Division of Environmental Protection
Department of Conservation and Natural Resources
375 E Warm Springs Rd, Suite 200
Las Vegas, NV 89119

Alan Pineda
Civil Engineer
Nevada Division of Environmental Protection
Department of Conservation and Natural Resources
375 E Warm Springs Rd, Suite 200
Las Vegas, NV 89119

Danielle D. Ward
Administrative Assistant
Nevada Division of Environmental Protection
Department of Conservation and Natural Resources
375 E Warm Springs Rd, Suite 200
Las Vegas, NV 89119

Steve Clough
Remediation Director
Nevada Environmental Response Trust
510 S. Fourth Street
Henderson, NV 89012

Alka Singhal
Senior Managing Consultant
Ramboll
2200 Powell St Suite 700
Emeryville, CA 94608

Nevada State Library and Archives
State Publications
100 North Stewart Street
Carson City, NV 89701-4285
NSLstatepubs@admin.nv.gov

Archives Getchell Library
University of Nevada, Reno
1664 N. Virginia St.
Reno, NV 89557
tradniecki@unr.edu

Document Section, Library
University of Nevada, Las Vegas
4505 Maryland Parkway
Las Vegas, NV 89154
sue.wainscott@unlv.edu

†Library
Southern Nevada Science Center
Desert Research Institute
755 E. Flamingo Road
Las Vegas, NV 89119-7363

All on distribution list receive one PDF copy, unless otherwise noted.

† 2 copies; CD with pdf (from which to print)